



## REDUCTIONS OF PRESSURE-DRAG-INCREASE AND FRICTION-DRAG DUE TO TURBULENT WATER FLOW OVER A SLIGHTLY SLIPPERY WAVY SURFACE

### Ryosuke Yamasaki

Department of Mechanical and System Engineering  
Kyoto Institute of Technology  
Matsugasaki, Sakyo-ku, Kyoto 606-8585, Japan  
george-r@k.vodafone.ne.jp

### Keisuke Maeda

Department of Mechanical and System Engineering  
Kyoto Institute of Technology  
Matsugasaki, Sakyo-ku, Kyoto 606-8585, Japan  
m3623049@edu.kit.ac.jp

### Atsuhide Kitagawa

Department of Mechanical and System Engineering  
Kyoto Institute of Technology  
Matsugasaki, Sakyo-ku, Kyoto 606-8585, Japan  
kitagawa@kit.ac.jp

### Yoshimichi Hagiwara

Department of Mechanical and System Engineering  
Kyoto Institute of Technology  
Matsugasaki, Sakyo-ku, Kyoto 606-8585, Japan  
yoshi@kit.ac.jp

### ABSTRACT

We have carried out velocity measurement for turbulent water flow over a slip-coat silicone rubber plate in an open channel at a high Reynolds number. This silicone rubber plate is a model of deformed skin of swimming dolphins. The friction drag acting on the plate has been estimated from the velocity profile. The total drag acting on the plate has been measured from the strain of thin metal strips supporting the plate. The experimental result shows 6.6 % reduction of total drag when compared with a conventional silicone rubber plate. We have also carried out an experiment using a hydrophilized polycarbonate wavy plate and have obtained 8.8 % reduction of friction drag compared with the slip-coat plate.

### INTRODUCTION

The reduction of drag acting on a moving body in fluid has been focused on for many years. The reduction of drag acting on a dolphin has also received a lot of attention. Several drag reduction mechanisms of dolphins, such as viscous damping by compliant skin, skin folds, propagation of skin deformation and skin separation, have been discussed (Fish, 2006; Endo and Himeno, 2002; Choi et al., 1997). One of the present authors observed the folds in a wide region of chest skin and abdominal skin which appear only when a bottlenose dolphin swims fast

(Zhang et al., 2007). Thus, the present authors think that the skin folds are related to the friction drag reduction mechanism. However, if the folded skins are considered to be a rigid wavy wall, the pressure drag and total drag increase noticeably with an increase in the ratio of amplitude to wavelength of the wavy wall (Henn and Sykes, 1999; Tuan et al., 2006). This increase decelerates the swimming speed of dolphins.

We carried out measurement of the drag acting on wavy silicone rubber plates in turbulent water flow in an open channel in our previous studies (Zhang et al., 2007; Ozaki et al., 2009; Kuroda et al., 2009). Silicone-rubber which was used in our previous studies is hydrophobic, and there are studies on reduction of drag by using hydrophobic surface. For example, the maximum drag reduction is estimated to be about 12 % on ribbon seal (Itoh et al., 2006) and the drag reduction was achieved using superhydrophobic surface treatments (Daniello et al., 2009; Peguero and Breuer, 2009). However, as far as we know, there is no paper on the reduction of drag by using a hydrophilic surface.

In the present study, we carry out measurements of flow and total drag acting on a slip-coat wavy plate and a hydrophilized polycarbonate wavy plate on the bottom of an open channel. The plates model the gradual motion of deformed skin or the gradual separation of skin surface of fast swimming dolphins.

## EXPERIMENTAL SETUP

### Apparatus

Figure 1 shows the apparatus. The apparatus is the same of those in our previous studies (Ozaki et al, 2009; Trieu et al., 2013). The open channel is 2000 mm in length and 270 mm in width. The bottom wall of the channel from the inlet to the downstream end of the test section was covered with a natural rubber sheet except for the area where the test plate was positioned. A tripping wire and emery paper were placed on the rubber sheet at the channel inlet in order to promote the development of a turbulent boundary layer flow. The  $x$  and  $y$  axes were configured in the streamwise and upward directions respectively. The test section was placed at  $1000 \text{ mm} < x < 1300 \text{ mm}$ .

The Reynolds number, based on the mean velocity  $u_e$  outside the turbulent boundary layer and the streamwise distance from the inlet of the channel, was  $1.2 \times 10^6$ . The Reynolds number based on  $u_e$  and the boundary layer thickness  $\delta_{995}$  was  $1.5 \times 10^4$ .

The Kolmogorov length scale  $l_K$  and Kolmogorov time scale  $t_K$  were estimated by using the friction velocity and the dissipation rate of turbulent kinetic energy. The dissipation rate near a flat wall was calculated from the DNS result obtained by Iwamoto et al (2002).  $l_K$  and  $t_K$  were 0.024 mm and 0.59 ms respectively.

### Test Plates

Figure 2 shows the test plate. This plate is similar to that used in our previous study. In this study, we prepared three test plates. One of them consists of a flat metal plate, narrow strips of double-sided adhesive tape and a thin silicone rubber sheet of 0.5mm in thickness. Second one consists of a flat metal plate, narrow strips of double-sided adhesive tape and a silicone rubber is coated with a thin slippery film, and is called Slip-coat rubber. This coating slightly increases the hydrophilicity of the surface. The third one consists of a flat metal plate, narrow strips of double-sided adhesive tape and a thin hydrophilized polycarbonate sheet - called hp - of 0.3 mm in thickness. This hp plate was used for examining the effect of hydrophilicity.

We measured contact angles for the plates. The contact angle was 92 degrees for the flat plate of the normal silicone rubber, while it was 77 degrees for the Slip-coat silicone rubber plate. The contact angle was 17 degrees for the hp plate.

The wavy surface was formed by inserting metal pipes between the base plate and the rubber film or hp sheet where the latter was not fixed by the tapes. The transverse width of the plate was chosen so that the pipes could be inserted into (or pulled out from) the test plate in the water channel. The total weight of the pipes was only 2 % of the total weight of the test plate. Thus the increase in weight caused by the insertion of the pipes to the plate was negligible. We confirmed that the shape of the rubber or sheet surface is sinusoidal-wavy. The wave amplitude  $a$ , and wavelength  $\lambda$ , were 0.7 mm and 20 mm respectively (See Figure 1(b)). The ratio,  $a/\lambda=0.035$ , is higher than the critical value for the appearance of flow separation regions in the case of rigid wavy walls (Tuan et al., 2006). For the discussion, we have divided the near-plate flow region

into the following six sub-regions as shown in Figure 3): valley, uphill1, uphill2, hilltop, downhill2 and downhill1.

A test plate without the insertion of pipes was used as a reference flat plate. Also, the plate with a normal silicone rubber sheet was used as an additional reference plate. The Reynolds number based on the bulk mean velocity and the water depth ( $=54\text{mm}$ ) was  $6.1 \times 10^4$ . The Reynolds number based on the friction velocity was  $2.6 \times 10^3$ .

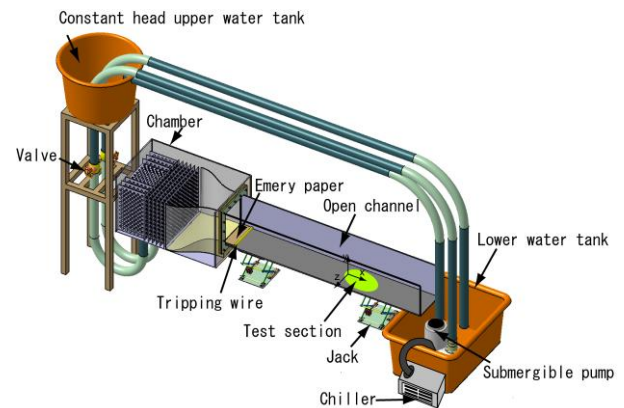


Fig. 1 Apparatus.

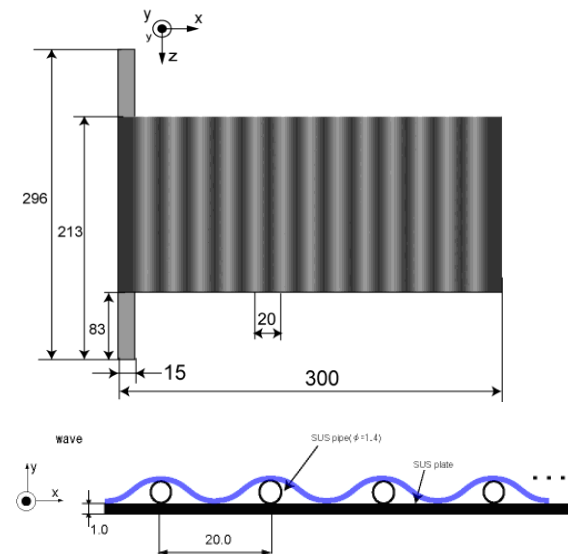


Fig. 2 Test plate: (a) configuration, (b) six sub-spaces.

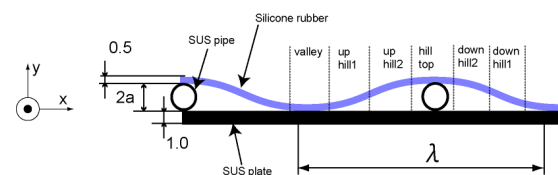


Fig. 3 Sectional view of wavy plate.

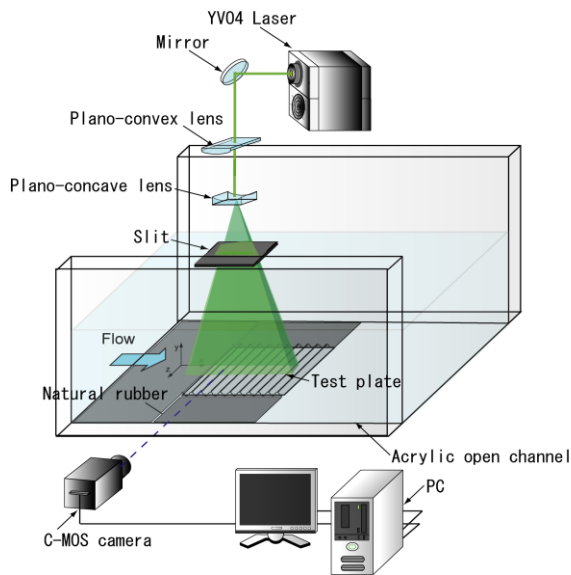


Fig. 4 Velocity measurement system

## MEASUREMENT PROCEDURES

### Velocity Field

We utilized tracer particles whose diameters were in the range of 0.050 - 0.060 mm, which is twice as large as  $l_K$ . The upper limit of the frequency  $f_r$ , beyond which these particles cannot respond to fluid sinusoidal fluctuations completely, was estimated to be 460 Hz from the equations obtained by Hjelmfelt Jr. and Mockros (1966). In addition, the frequency corresponding to the velocity fluctuation due to the smallest eddies can be expressed by the reciprocal of the Kolmogorov time scale, which is  $1/t_K = 1700$  Hz.  $f_r$  is lower than  $1/t_K$ . This shows that the particles cannot respond to fluctuations caused by the smallest eddies. However,  $f_r$  is nearly the same as the frequency of flow fluctuation, which can be captured by the camera mentioned below. Thus the tracer particles adopted in the present study are reasonable.

The measurement system is shown in Figure 4. The light of an Nd: YVO<sub>4</sub> laser was used as the light source. The laser beam was expanded with a plano-convex cylindrical lens and a plano-concave lens. The laser light passed through a slit of 5 mm in width above the free surface. The laser light sheet thus obtained illuminated the flow. The test plate was fixed on the bottom wall of the test section.

Scattered light from the particles was captured with a CMOS camera (Photron, FASTCAM 1024-PCI). The camera was located at one side of the channel as shown in Figure 4. The optical axis of the camera was set parallel to the ridgelines of the wavy plates so that the valleys of the plates could be observed completely. The frame rate was 1000 fps and the pixel covering area was  $0.0291 \times 0.0291$  mm<sup>2</sup>. The captured images were directly recorded into the memory of an interface board in a PC.

We adopted the following three-step processing of images, which is the same as that adopted in our previous studies (Kitagawa et al., 2007, Trieu et al., 2013):

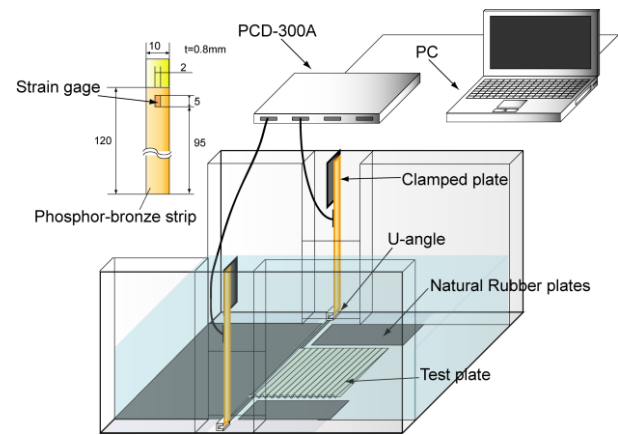


Fig. 5 Measurement system of total drag

(1) The particle-mask correlation method, developed by Etoh et al., (1999), was used to remove any weak scattered light from particles in the images.

(2) The PTV (Particle Tracking Velocimetry) technique based on the velocity gradient tensor method, proposed by Ishikawa et al., (2000), was applied to the preprocessed images for obtaining velocity vectors. In this method, the matrix including the velocity gradient tensor was calculated for pairs of neighboring particles in a specific region around a single particle.

(3) Then, the sum of the square of errors in the matrix was evaluated.

This procedure was repeated for all the candidate particles until the sum reached its minimum value. This method has the advantage of accurately reproducing strongly-deformed velocity fields.

The velocities of the particles were redistributed to the grid points of  $14 \times 50$ . The velocity of a particle was simply shifted to the nearest grid point in the redistribution procedure. The uncertainty of the velocity was 0.012 m/s for  $u_c=1.14$ m/s. This shows that the measured velocity was accurate.

### Total drag

When the total drag was measured, the test plates were not fixed to the bottom wall. Many particles of 0.3 mm in diameter were arranged between the lower surface of the test plate and the surface of the channel in order to reduce the friction force between the test plate and the bottom of the channel.

The measurement system for the total drag acting on the test plate is indicated in Figure 5. The test plate was supported by two vertical cantilevers, which were made of phosphor-bronze strips. One end of each cantilever was clamped above the free surface. The other end of each cantilever made contact with one of the edges of a U-shaped mini channel. This mini channel was fixed to the edge of each wing of the test plate. The cantilevers were deflected slightly by the movement of the test plate due to the total drag acting on the plate. Since the measurement

of the deflections in water flow is difficult, we measured the strain at the location of each cantilever by using a strain gauge. The gauges were attached to the cantilevers and connected to bridge circuits. The outputs from the circuits were recorded on a PC. In order to reduce errors caused by the flow which collides with the cantilevers, the cantilevers were positioned inside the indented parts of the sidewall.

We carried out a calibration in order to obtain the relationship between the output from the strain gauges and the deflection of the cantilever at the loading line (i.e. the contact line of the edge of the mini channel). The cantilever was held horizontally in the air. Weights were used for changing the load at the loading line. The deflection was measured with a laser displacement sensor. The force acting on the cantilever was calculated from the deflection, the length of the cantilever and Young's modulus. The error for the total drag was approximately  $\pm 1.3\%$ .

## RESULTS AND DISCUSSION

### Velocity field

**Flat plate.** Figure 6 shows the profile of mean streamwise velocity. The mean velocity for the Slip-coat flat plate is in agreement with that for the normal silicone rubber flat plate. The friction velocity was calculated from the gradient of mean velocity. The gradient was obtained from the fitting curve expressed with a fourth-order least square polynomial.

The Reynolds shear stress was measured by Klebanoff (in Schlichting, 1979) as shown in Figure 7. The Reynolds shear stress of the Slip-coat is lower than that of the Normal near the test plate.

**Wavy plates.** The mean velocities in the valley region are shown in Figures 8 and 9. (Hereafter, the friction velocity of the flat plate is used for the non-dimensional form of velocity). In the valley region, the mean velocities near the surface of hp are lower than for Slip-coat. Thus the mean velocity was affected by the hydrophilicity of wavy surfaces.

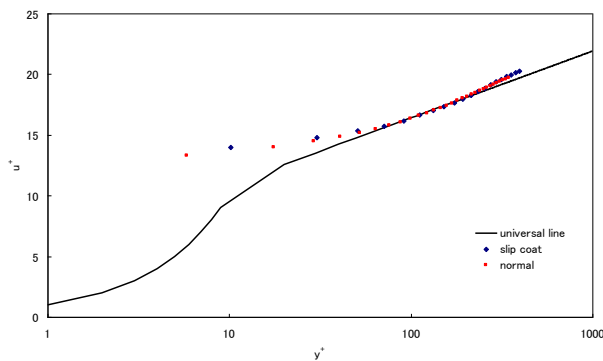


Fig. 6 Mean velocity profile for flat plate.

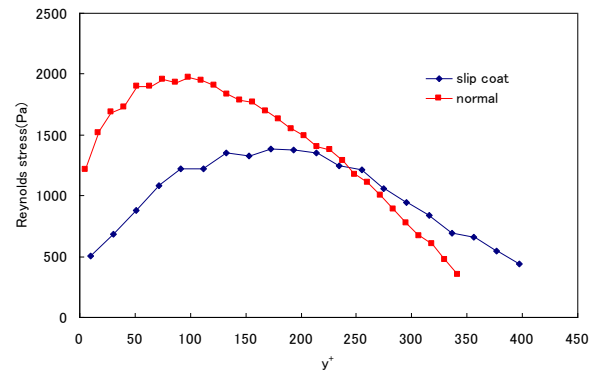


Fig. 7 Reynolds stress profiles in the case of the flat plate.

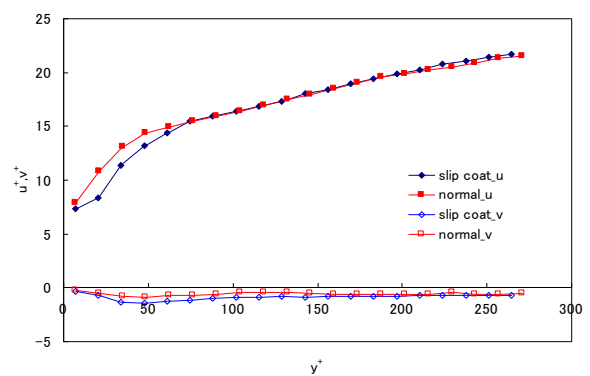


Fig. 8 Mean velocity profiles in the valley region in the case of Normal and Slip-coat.

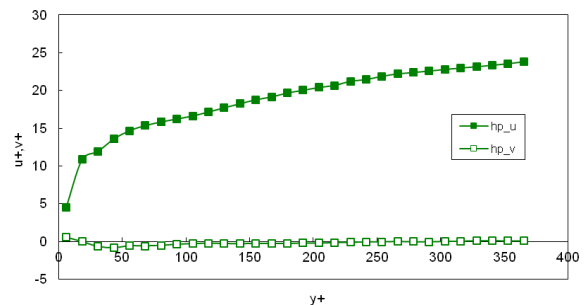


Fig. 9 Mean velocity profiles in the valley region in the case of hp.

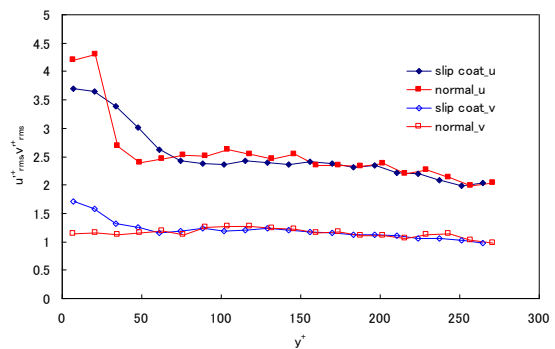


Fig. 10 Turbulence intensity profiles in the valley region in the case of Normal and Slip-coat.

Table. 1 Wall shear stress  $\tau_w$ (Pa)

	Normal	Slip-coat	hp
valley	2.12	2.01	1.67
uphill 1	2.21	2.12	2.11
uphill 2	2.74	2.65	2.21
hilltop	2.91	2.86	2.70
downhill 2	2.85	2.75	2.50
downhill 1	2.41	2.31	2.21
Average	2.54	2.45	2.23

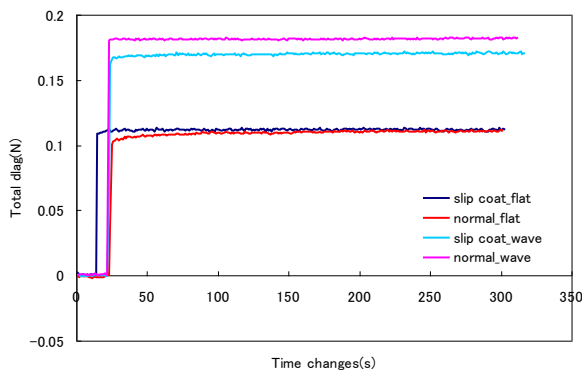


Fig. 11 Time changes in total drag in the case of Normal and Slip-coat.

The turbulence intensities in the streamwise and vertical directions in the valley region are shown in Figure 10. The vertical intensities of Slip-coat are higher than those for Normal in the valley region near the plate. This is probably because the recirculation flow, which occurs in Slip-coat in the valley region, occurs more greatly or more frequently than for Normal.

**Wall shear stress.** Table 1 shows the wall shear stress which is calculated for the six sections by the Clauser method (Clauser, 1956). The wall shear stress of the Slip-coat wavy plate is 3.5% lower than that of the normal wavy plate. This decrease of wall shear stress does not depend on the sub-region except for the hilltop.

It is found from Table 1 that the wall shear stress of the hp wavy plate is 8.8% lower than that of the Slip-coat silicone rubber. The decrease of wall shear stress is noticeable in the valley region. This may be due to the modification of recirculation flow.

**Total drag.** Figure 11 shows the total drag of the Normal and Slip-coat. The time-averaged value of the total drag for the flat plate is 0.11N. The total drag should be equal to the friction drag acting on the flat plate. By assuming that the mean velocity profile is uniform over the whole surface of the flat plate, one can calculate the friction drag from the friction velocity. It was 0.11N. Thus, the measured values of total drag and friction velocity are reasonable in the case of the flat plate in the present study.

The time-averaged value of the total drag for the Normal is 0.18 N and for the Slip-coat is 0.17N. Thus, the total drag of the wavy plate made of Slip-coat silicone rubber is 6.6% lower than that of the normal silicone rubber.

The pressure drag was estimated from the difference between the total drag and the friction drag. The pressure drag of the Slip-coat wavy plate was 0.96N, while the pressure drag of the normal wavy plate was 0.099N. Thus, the former is 3.0% lower than that of the latter.

The pressure drag for the hp wavy plate was not lower than that for the Slip-coat wavy plate. This is probably owing to the difference in the elasticity of the plates.

## CONCLUSIONS

Measurements were conducted for the velocity field of turbulent boundary-layer flow along the wavy plates and the total drag acting on these plates. The main conclusions obtained are as follows:

- (1) The wall shear stress of the wavy plate made of Slip-coat silicone rubber is 3.5% lower than that of the normal silicone rubber. This decrease of wall shear stress does not depend on the sub-region except for the hilltop.
- (2) The total drag of the wavy plate made of Slip-coat silicone rubber is 6.6% lower than that of the normal silicone rubber.
- (3) The pressure drag, estimated from the difference between the total drag and the friction drag, of the wavy plate made of Slip-coat silicone rubber is 3.0% lower than that of the normal silicone rubber.
- (4) The wall shear stress of the wavy plate made of the hydrophilized polycarbonate is 8.8% lower than that of the Slip-coat silicone rubber. Thus, the hydrophilic wavy surfaces are effective for the reduction of friction drag.

## ACKNOWLEDGMENTS

The authors thank Mr. M. Shintani at Yamamoto Kogaku Co., Ltd. for his supply of hydrophilized polycarbonate plates.

## REFERENCES

- Choi, K. -S., et al., 1997, "Turbulent drag reduction using compliant surfaces", *Proceedings of Royal Society of London A*, 453, pp. 2229-2240.
- Clauser, F. H., 1956, "Turbulent Boundary Layers", *Advances in Applied Mechanics*, Vol. IV, pp. 1-51.
- Daniello, R. J. et al., 2009, "Drag reduction in turbulent flows over superhydrophobic surfaces", *Physics of Fluids*, Vol. 21, pp. 085103-1 – 085103-10.
- Endo, T. and Himeno, R., 2002, "Direct numerical simulation of turbulent flow over a compliant surface", *Journal of Turbulence* Vol. 3, article no. 007, pp. 1-10.
- Etoh, T., Takehara, K. and Okamoto, K., 1999, "Performance evaluation of the PMC and the KC methods for particle extraction and tracking through their application to standard particle images" (in Japanese), *Transactions of Japan Society of Mechanical Engineers*, Vol. 65, Ser. B, pp. 1688-1695.

Fish, F. E., 2006, "The myth and reality of Gray's paradox: implications of dolphin drag reduction for technology", *Journal of Bio-mimetics and Bio-inspiration*, Vol. 1, pp. R17-R25.

Henn, D. S., and Sykes, R. I., 1999, "Large-eddy simulation of flow over wavy surfaces", *Journal of Fluid Mechanics*, Vol. 383, pp. 75-112.

Hjelmfelt Jr, A. T. and Mockros, L. F., 1966, "Motion of discrete particles in a turbulent fluid", *Applied Scientific Research*, Vol. 16, pp. 149-161.

Ishikawa, M. et al., 2000, "A novel algorithm for particle tracking velocimetry using the velocity gradient tensor", *Experiments in Fluids*, Vol. 29, pp. 519-531.

Itoh, M. et al., 2006, "Turbulent drag reduction by the seal fur surface", *Physics of Fluids*, Vol. 18, pp. 065102-1-065102-9.

Iwamoto, K., Suzuki, Y. and Kasagi, N., 2002, "Reynolds number effect on wall turbulence: toward effective feedback control", *International Journal of Heat and Fluid Flow*, Vol. 23, pp. 678-689.

Kitagawa, A., Hagiwara, Y., and Kouda, T., 2007, "PTV investigation of phase interaction in dispersed liquid-liquid two-phase turbulent swirling flow", *Experiments in Fluids*, Vol. 42, pp. 871-880.

Kuroda, T., Yoshitake, N., Ozaki, Y., Hagiwara, Y. and Kitagawa, A., 2009, "Turbulence and drag associated with water boundary-layer flow over plates at a high Reynolds number", *Turbulence, Heat and Mass Transfer* 6, pp. 959-962.

Ozaki, Y. Yoshitake, N. and Hagiwara, Y., 2009, "Drag acting on an angled-wavy plate by turbulent water flow at a high Reynolds number", *Proceedings of 6th International Symposium on Turbulence and Shear Flow Phenomena*, Vol.2, pp.771- 776.

Peguero, C. and Breuer, K., 2009, "On drag reduction in turbulent channel flow over superhydrophobic surfaces", *Advances in Turbulence XII*, pp. 233-236.

Schlichting H., 1979, *Boundary-Layer Theory*, McGraw Hill, New York.

Trieu, D. C., Ymasaki, R. and Hagiwara, Y., 2013, "Drags acting on a wavy plate with symmetrical ridgelines simulating folded skins of dolphins", *Journal of Aero Aqua Bio-mechanisms*, Vol. 3, No. 1, pp. 29-35.

Tuan, H. A., El-Samni, O., Yoon, H. S., and Chun, H. H., 2006, "Immersed boundary method for simulating turbulent flow over a wavy channel", *Extended Abstracts of Whither Turbulence Prediction and Control*, pp. 116-117.

Zhang, H., Yoshitake N. and Hagiwara, Y., 2007, "Changes in drag acting on an angled wavy silicone-rubber plate as a model of the skin folds of a swimming dolphin", *Bio-mechanisms of Animals in Swimming and Flying*, Springer Verlag, Tokyo, Chapter 8, pp. 91-102.